

# Inner Control Loops Approach to Control the Islanded Photovoltaic Microgrid

Guy Wanlongo Ndiwulu, Emmanuel De Jaeger, Angelo Kuti Lusala  
 Mechatronic, Electrical Energy, and Dynamic Systems (MEED)  
 Université catholique de Louvain (UCL)  
 Louvain-la-Neuve, Belgium  
 {guy.wanlongo, emmanuel.dejaeger}@uclouvain.be

**Abstract**—The intermittent character of the photovoltaic generator, power electronic converters and load dynamic are the main factors leading operation instability in islanded microgrids. The necessity of the immediate control within the micro-source is very important since it impacts the interaction between micro-sources in the microgrid. This control level must be characterized by a fast and accurate response in order to control the operation point of the photovoltaic generator of the microgrid, and also the injected currents into the microgrid, as well as the amplitude and the frequency of the voltage at the photovoltaic connecting point at AC side. However, its performance depends on the control structure and the connecting mode of the photovoltaic generator. In this present paper, we propose a new structure of the internal control applied in islanded photovoltaic microgrids. It advocates the use of the close control multi-objective controller which is developed and implemented with Matlab/Simulink. Accordingly, the simulation results obtained show that this control approach improves the stability operation of the islanded microgrid while allowing maximum power transfer from DC to AC side.

**Keywords**—Islanded Microgrid, Photovoltaic, Close Control, Power Converters.

## I. INTRODUCTION

The islanded microgrids are characterized by a low-voltage three-phase or single-phase system composed of micro-sources, energy storage devices, loads and control system. They represent credible technological alternative solutions to solve the problem of the energy access in remote areas of developing countries, chiefly in Africa. As such they help improve the electrification conditions, develop clean energy and avoid or decrease greenhouse gas emissions, - as has always been the case with our dependence on the diesel generator. The micro-sources into the islanded microgrids may be multiple and miscellaneous [1]-[5]. The photovoltaic generator (PVG) may be considered as one of the greatest energy potential in Africa, and it can be valorized within these islanded systems. Nevertheless, the intermittent character of this micro-source can have a negative impact on the voltage and frequency stability of the microgrids [1]-[5]. Likewise, the load variation is another major factor which can make the islanded microgrids little stable [6]. These require a control system to stabilize the operation of the microgrid. The control strategies applied within these systems should have very specific characteristics in order to preserve the integrity and the stability of the voltage and frequency. The control system itself needs a short time response in order to maintain the integrity of the microgrid and to quickly restore the frequency and voltage during an early timing of the disturbances. Acceptable performances can be obtained through adequate inner control loops for the photovoltaic converter [6]. The structure of this controller also depends on the connecting mode of the photovoltaic generator, the architecture of the microgrid and the control flexibility of the system. Two connecting modes are often considered in the scientific literature [7]-[11]. In the first one [9]-[12], the photovoltaic generator (PVG)

is first of all connected to the grid via an inverter. At the DC side, it is connected in parallel with a battery; both of which feed the loads through the same inverter. This approach is the most intensely studied connecting mode, and it allows to make an account for transient solar conditions. In addition, the DC-DC converter can be used to realize, when needed the maximum power point tracking (MPPT) of the PVG. However, this mode proves none too reliable during the operation. In the second connected mode, the PVG feeds the AC load via an inverter as described in [7] and [13]. The immediate inconvenience with this approach is that it does not take into account the intermittent character of the irradiance.

These connection modes are also characterized by voltage inverters, and a specific control mode. The control of the amplitude and frequency of the voltage (V-f control) is often used as the control mode serving to stabilize the voltage within the microgrid [9]-[13]. This controller is frequently made in the synchronous reference frame, and can be characterized by a control algorithm constituted of one or two inner control loops. The control algorithm with one inner control loop, mostly used, is composed of direct and quadrature components of the voltage loops. And it can be adapted for the islanded systems with single connecting point, without elementary distribution system. Nonetheless, this control structure gives less control flexibility of the power transferred from the PVG to the AC side.

From the on-going, we notice that none of the aforementioned studies deals with the case of the two independent inverters: PVG inverter and battery inverter. However, this issue has a considerable influence on the connecting mode and control mode of the PVG. This can enhance the reliance on the islanded microgrid. In effect by using a mixed internal control, it can provide significant benefits on the power transfer control while efficiently regulating the amplitude and the frequency of the AC voltage. By mixing both modes, i.e., the active and reactive power (PQ), and V-f ones, we respectively ensure at the same time the control of the injected currents and that of the amplitude and the frequency of the voltage within the microgrid. This paper presents an inner control loops approach which controls the islanded photovoltaic microgrid with two independent inverters. This control strategy is implemented in the synchronous reference frame, and applied to the photovoltaic inverter and the battery inverter. It consists in controlling the power transfer from the PVG to the grid, and the amplitude of the grid voltage. The PQ control mode is used in the first inverter to control the direct and quadrature components of the currents it injects into the grid. Also, the V-f control mode is applied to the battery inverter to regulate the direct and quadrature components of the grid voltage. In addition, this control approach provides the particularity of developing the PQ control within the islanded microgrid with the advantage of accomplishing a maximum power transfer control from the PVG. And it also provides the

possibility to integrate other control levels. This paper assumes a balanced three-phase system and three-phase voltage inverters.

The remainder of the paper is organized as follows: section II gives a brief description of the related works. Section III presents an inner control loops approach developed for the photovoltaic generator connected to a microgrid. This, in turn encompasses the maximum power point tracking (MPPT), PQ and V-f controllers. Section IV treats the performance analysis of the multi-objective controller by simulation. Last but not least, section V gives some conclusion including future research steps.

## II. RELATED WORKS

The application of the close control within an islanded photovoltaic microgrid with two independent inverters can be an interesting way of providing an efficient internal control flexibility and may allow an optimal exploitation of the photovoltaic. It also provides more flexibility of coordination than does the centralized inverter, because the mixed PQ and V-f control can be applied to assure both power control and voltage stability. But, scarce are the papers which examine this control approach and its implementation.

In [7], the authors deal with the primary and secondary control strategies for photovoltaic power plants in islanded microgrids to control the voltage and the frequency. The simulation results show that this proposed approach efficiently regulates the voltage and frequency. But, the influence of control strategies on the maximum power transfer from the photovoltaic to the AC side is not examined. Also, the internal control approach is not considered. In [13], three-phase islanded photovoltaic microgrid with variable load is considered. The voltage stability of the system is controlled with an internal control. However, the power control is not investigated. Reference [9] investigates the implementation of a TS-fuzzy controller to regulate the DC voltage of the inverter to maintain both the amplitude and the frequency of its output voltage. The system used by these authors is composed of a photovoltaic generator, a diesel generator, a battery and the loads. However, the photovoltaic and the battery are connected to loads through a centralized inverter. The V-f mode is applied to control the inverter but no power transit issues have been investigated. Reference [14] presents an investigation of the dynamic modelling of a hybrid system constituted of a photovoltaic, a battery and DC loads. Conversely, it does not study the internal control issues of the microgrid. In [10], the modelling and dynamic performances of an islanded system formed by a photovoltaic, a battery and loads are analyzed. The results obtained show that the V-f control mode regulates efficiently the amplitude and the frequency of the voltage. Centralized inverter is also used. Nevertheless, no maximum power transfer issues are addressed. In [12], the islanded hybrid photovoltaic using the centralized inverter is proposed. Internal control is implemented to control the DC voltage as well as the amplitude and the frequency of the voltage. The simulation results prove that the controller performance is satisfactory under transient solar and load power conditions. Herein, the control of system stability is achieved by a centralized inverter. Reference [11] proposes V-f control based on a fuzzy logic controller to control an islanded microgrid. However, a centralized inverter is used to connect a photovoltaic, a solid oxide fuel cell and a battery.

## III. PROPOSED APPROACH

### A. Islanded microgrid architecture

Fig. 1 below shows the low-voltage three-phase islanded microgrid architecture, constituted of a photovoltaic generator, a battery, a boost converter, two voltage inverters, two filters, two lines and loads. The

converters DC-DC and DC-AC are used respectively to make the maximum power point tracking (MPPT) and to make usable the electric power supplied to the AC loads. The two voltage inverters have very specific control roles: the photovoltaic inverter to control the powers, and the battery inverter to assure the voltage amplitude. Both feed the loads at the point of common coupling.

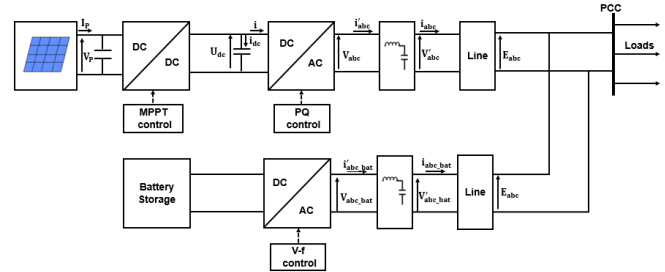


Fig. 1. Islanded microgrid architecture

### B. Modelling of the microgrid components

1) *Photovoltaic generator*: The electrical models of the photovoltaic are found in the [15], [16]. The simplified equivalent scheme of the model with one diode is given in Fig. 2. The output current of the cell is given by (1).

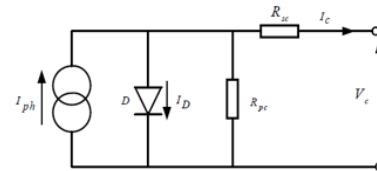


Fig. 2. Equivalent scheme of the photovoltaic cell

$$I_C = I_{ph} - I_0 \left[ \exp \left( \frac{q}{mKT_C} (V_C + R_{sC}I_C) \right) - 1 \right] - \frac{V_C + R_{sC}I_C}{R_{pC}} \quad (1)$$

Where,  $I_{ph}$  is the photocurrent,  $I_0$  is the saturation current,  $q$  is the electron charge,  $T_c$  is the temperature of the cell,  $m$  is the solar cell ideality constant,  $K$  is the Boltzmann constant,  $V_C$  the cell voltage,  $R_{sC}$  is the series resistance,  $R_{pC}$  is the parallel resistance (Fig. 2). The output current of the photovoltaic generator  $I_P$  is characterized by the number of parallel  $N_p$  and series  $N_s$  modules, cells connected in series  $n_s$ , and output voltage of the PVG  $V_P$ . It is given by:

$$I_P = N_P I_{ph} - N_P I_0 \left[ \exp \left( \frac{q}{KkT_C} \left( \frac{V_P}{n_s N_s} + \frac{R_{sC} I_P}{N_P} \right) \right) - 1 \right] - \frac{N_P}{R_{pC}} \left( \frac{V_P}{n_s N_s} + \frac{R_{sC} I_P}{N_P} \right) \quad (2)$$

2) *Modelling of the inverter*: The modelling of the three-phase Pulse Width Modulation (PWM) inverter in the microgrid environment is detailed in [9], [17], [18]. Equations (3) and (4) give the modelling of the inverter in the  $d-q$  referential. The LC filter and the  $R + jX$  impedance line are taken into account in the modelling (see Fig. 1).

$$V_d = E_d + R i_d + L \frac{d i_d}{dt} - \omega L i_q \quad (3)$$

$$V_q = E_q + R i_q + L \frac{d i_q}{dt} + \omega L i_d \quad (4)$$

Where,  $V_d$  and  $V_q$  are the direct and quadrature components of the voltage at the output of the inverter voltage,  $R$  is the resistance of the

microgrid,  $L$  is the microgrid inductance,  $E_d$  and  $E_q$  are the direct and quadrature components of the voltage at the point of common coupling (in Fig. 1).

3) *Modelling of the boost converter*: The boost converter is very important to make the maximum power point tracking of the photovoltaic power (see Fig. 3). Its modelling depends on the two operating sequences which are represented by differential equations (5) and (6) [12], [13]. Where  $L$  and  $D$ , are the boost inductance and the duty cycle respectively.

$$L \frac{di_{PV}}{dt} = V_{PV} - (1 - D) U_{dc} \quad (5)$$

$$C \frac{dU_{dc}}{dt} = (1 - D) i_{PV} - i_d \quad (6)$$

4) *Modelling of the energy storage battery*: The battery is modelled to feed the inverter in constant DC voltage. We find a large variety of the battery models in the scientific literature [19]-[21]. All models represent the battery by an electric circuit, composed of a resistance, a capacitance and other elements which depend on the battery state of charge (SOC) and the temperature. However, the simplified model is considered in this paper. It is made up of a series resistance and a controllable voltage source, given by (7) [20].

$$E = E_0 + K \frac{Q}{Q + \int (i_b) dt} + A \exp(-B \int (i_b) dt) \quad (7)$$

Where,  $E$  is the no-load voltage,  $E_0$  is the battery constant voltage,  $K$  is the polarization voltage,  $Q$  is the battery capacity,  $\int (i_b) dt$  is the actual battery charge,  $A$  is the exponential zone amplitude, and  $B$  is the exponential zone time constant inverse.

### C. Structure of the inner control loops

The structure of the inner control loops multi-objective controller is shown in Fig. 3. It allows the immediate control of the electronic power converters in order to regulate the current and voltage of the photovoltaic generator, as well as the input DC voltage of the inverter and the transfer of the power from the PVG. Besides, it also controls the amplitude and the frequency of the voltage at the point of common coupling. However, the boost converter is used to control the photovoltaic variables by implementing the MPPT. By applying the PQ control mode to photovoltaic inverter, we control the DC voltage and power transit. And by applying the V-f control mode to the battery converter, we regulate both the amplitude and frequency of the voltage at the AC side.

1) *Maximum power point tracking (MPPT)*: Many techniques of the MPPT may be found in the literature [22], all of which presenting the pro's and con's. In this paper, we use the Perturb and Observe method [22]. This algorithm is illustrated by Fig. 4. It is based on the small disturbance of the photovoltaic current or voltage and, on the measurement observation of the power.

2) *PQ controller structure*: The proposed PQ controller mitigates the influence of intermittent character at the inverter input by controlling the DC voltage. It also ensures the transfer of the maximum power from the photovoltaic installation to the AC grid by controlling the currents injected by the inverter. However, the implementation of this controller in an islanded system requires another converter for securing the amplitude and the frequency of the voltage. For that purpose, the battery inverter is piloted in V-f control mode.

a) *Modelling of the PQ controller*: The DC voltage of the photovoltaic inverter may be formulated by the power balancing at the converter input (see Fig. 3). This is given by:

$$CU_{dc} \frac{dU_{dc}}{dt} = P_{PV} - P_{AC} \quad (8)$$

The equation (8) can be rewritten in Laplace domain as follows:

$$U_{dc}^2 = \frac{P_{PV} - P_{AC}}{Cs} \quad (9)$$

Equations (8) and (9) show that the square of the inverter DC voltage is proportional to the power difference between the photovoltaic and AC side of the inverter. To transfer the maximum power from the photovoltaic. The input DC voltage variation should be minimal. The active and reactive powers injected by the inverter can be calculated by (10) and (11). Similarly, the Phase Locked Loop system sets the frequency and, forces the quadrature component of the voltage at the point of common coupling to get zero value.

$$P = \frac{3}{2} E_d i_d \quad (10)$$

$$Q = -\frac{3}{2} E_d i_q \quad (11)$$

The decoupling of the two components shows that the active and reactive powers produced by the PVG may be regulated via the injected currents in the inverter.

b) *Algorithm of id and iq control*: The control algorithm of id and iq is given by the Fig. 5. It is made of two cascades of proportional and integral controllers (PI). The external loop regulates the powers and the internal one controls the currents. This control is conducted in the synchronous reference frame with a decoupling between the direct and the quadrature components. Also, the reference of the direct component of current is provided by the power controller. The set point of this controller is the difference between the square of the measured DC voltage, and that of the reference value. The reference voltage value corresponds to the maximum power point of the PVG.

The reference of the quadrature component of the current is supplied by the reactive power. The reference value of this power depends on the microgrid state. Besides, the feedforward terms are added to the output of the current controllers.

The instantaneous angle for the Park transformations is provided by Synchronous Frame Phase Locked Loop (SF-PLL) [23]. Finally, the inverter receives the control signals via the Pulse Width Modulation.

3) *V-f controller structure*: It is responsible for maintaining the amplitude and the frequency of the voltage at the common coupling point.

The structure of this controller is shown in Fig. 6. It is constituted of two cascades of PI controllers. The external loop controls the direct and quadrature components of the voltage. It also provides the set point of currents to the internal loop.

The control loop of currents regulates the output currents of the inverter. We add the currents feedforward terms while considering the effect of the line.

Furthermore, this controller regulates only the voltage amplitude while the voltage frequency is assigned at 50Hz. It is supplied to the Park transformations by an integrator. The reference voltages are given below.

$$E_d^* = \frac{U_{dc}}{\sqrt{3}} \quad E_q^* = 0 \quad \theta = \int w^* dt$$

4) *Design of the PIs controllers*: The design of proportional and integral controllers is carried out with the analytical method based on the canonical form of the transfer function of the second order at closed loop. The resulting gains of the controllers are given in Table I.

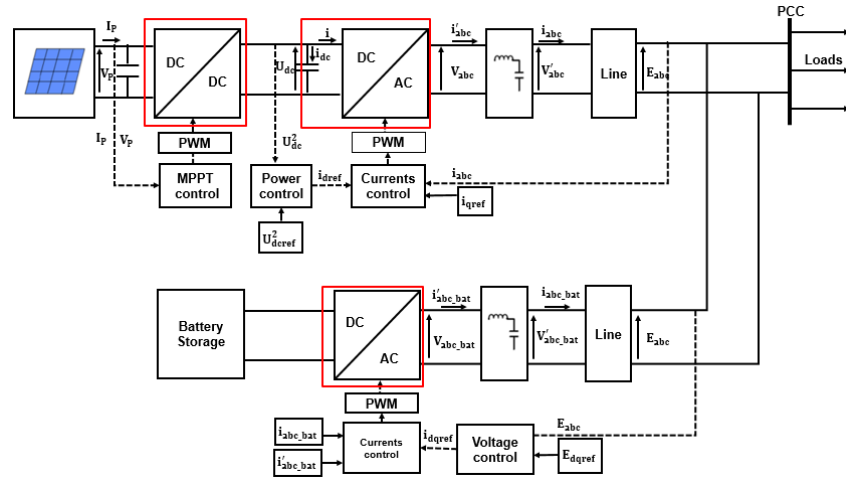


Fig. 3. Structure of the inner control loops

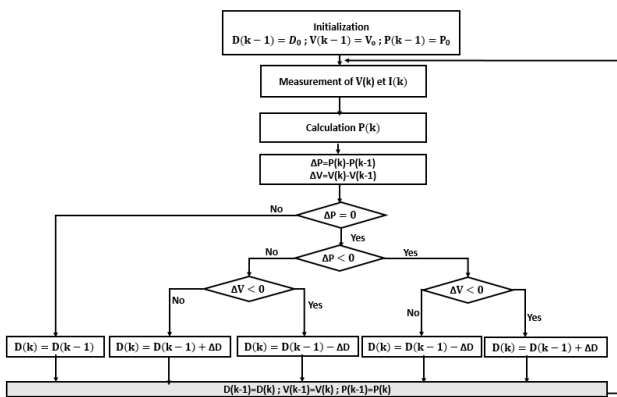


Fig. 4. Algorithm of Perturb and Observe method

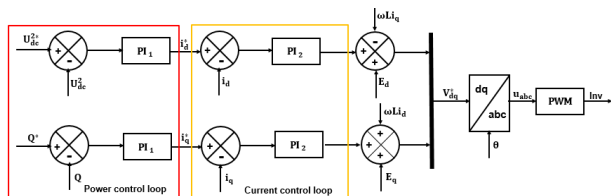


Fig. 5. Algorithm of current controllers in the synchronous reference frame

TABLE I  
CONTROLLERS GAINS WITH THE ANALYTICAL METHOD

Control mode	External gains	Internal gains
PQ Control	$K_P = \frac{-2\zeta\omega C}{E_d}$ ; $K_I = \frac{C\omega^2}{E_d}$	$K_P = 2\zeta\omega L - R$
V-f Control	$K_P = \frac{2\zeta\omega L - R}{K}$ ; $K_I = \frac{L\omega^2}{K}$	$K_P = 2\zeta\omega L - R$

IV. SIMULATION RESULTS

The proposed approach is studied through Matlab/Simulink simulations. The output parameters as characteristics of photovoltaic, DC voltage, direct and quadrature components of the current, direct and quadrature components of the voltage, voltage amplitude, and active power, are plotted and analyzed considering three scenarios. The parameter values of islanded microgrid are given in Table II.

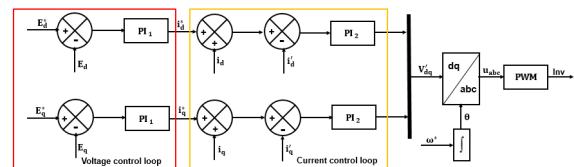


Fig. 6. Algorithm of voltage amplitude control in the synchronous reference frame

TABLE II  
PARAMETERS VALUES OF THE SYSTEMS COMPONENTS

PV: SunPower SPR-305-WHT	Inverter
$n_s=9; N_s=9; N_p=18; I_{sc}=9.96A; V_{oc}=64.2V$	$K=1; U_{rms} = \frac{U_{dc}}{\sqrt{2}}$
LC Filter	Line(Ω/km)
$L_f=5000\mu H; C_f=300\mu F; R_d=0.531\Omega$	$R=0.65; X=0.025$
DC Bus	
$U_{dc}=V_{PV}; C=500\mu F$	

A. First scenario: Irradiance and loads are steady

Fig. 7a and 7b illustrate the output current and voltage of the photovoltaic, as well as the DC voltage of the inverter. These results show that the photovoltaic generator operates to its maximum power. The DC voltage is maintained at the reference value representing a maximum power point. The results of the injected currents are given in Fig. 8a and 8b. Therefore, we can notice that the quadrature component is zero. This is due to the reference value of the reactive power which is equal to null. Fig. 9a shows that the maximum power produced by the photovoltaic generator is completely transferred to the AC side. This is the particularity of this control approach. Besides, Fig. 10a and 10b give the direct and the quadrature components of the voltage. These results correspond effectively to the reference values imposed by the V-f controller. Moreover, the amplitude of the voltage at the point of common coupling is given by Fig. 11a. Fig. 9b shows that the voltages are well balanced as was inferred.

B. Second scenario: Constant irradiance with variation loads

By disconnecting one of the loads between 2s and 3s, we create the disturbances in the microgrid. And this, in turn, brings about the

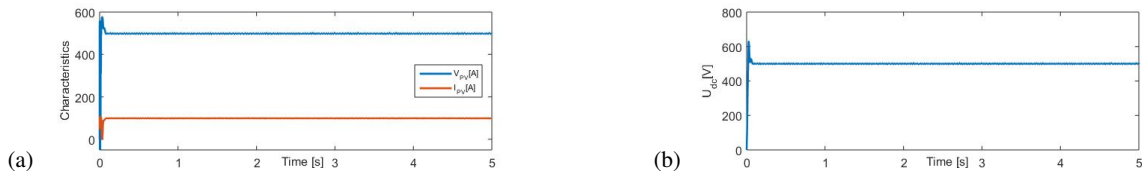


Fig. 7. Operation characteristics of the photovoltaic (a) and DC inverter voltage (b), by considering the first scenario.

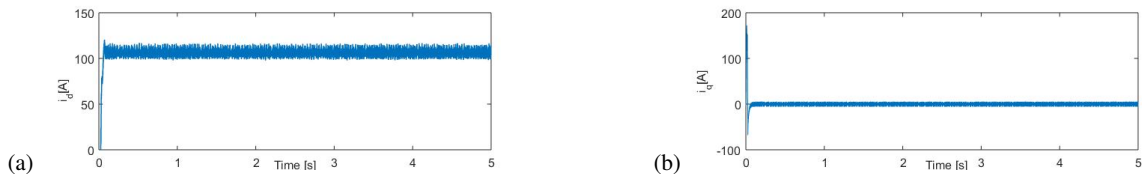


Fig. 8. Direct and quadrature components of the currents injected by the photovoltaic inverter (a and b), by considering the first scenario.

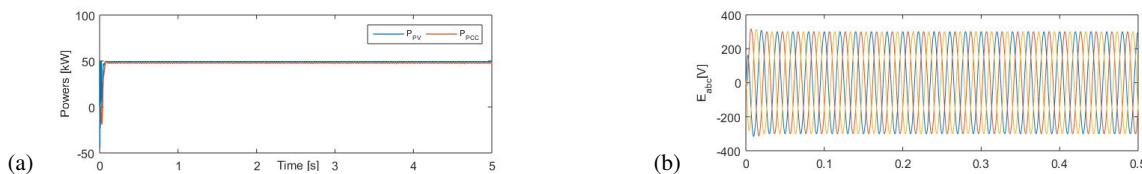


Fig. 9. Power balancing (a) and three-phase voltage systems (b), by considering the first scenario.

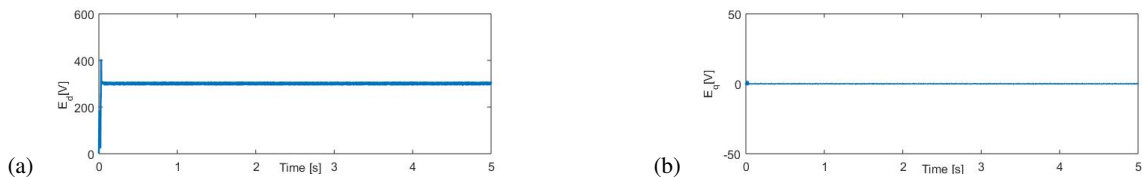


Fig. 10. Direct and quadrature components of the measure PCC voltage (a and b), by considering the first scenario.

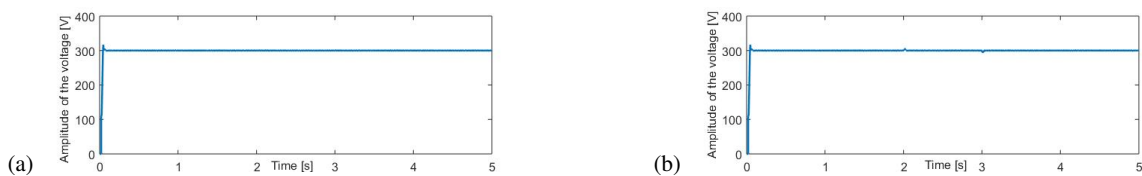


Fig. 11. Amplitude of the voltage at the PCC by considering the first scenario (a) and the second scenario (b).

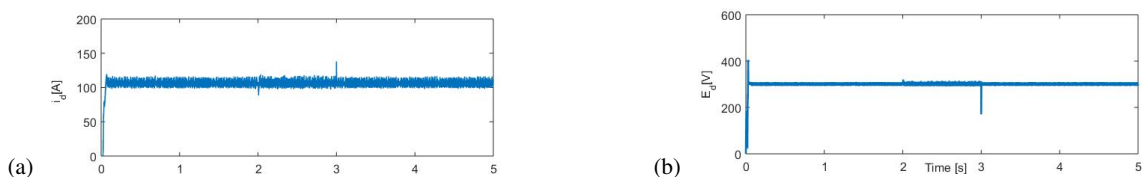


Fig. 12. Direct component of the current (a) and the voltage (b), by considering the second scenario.

controller reaction. This disconnection involves the decreasing of the current and the increasing of the voltage amplitude at the point of common coupling. The injected current is shown by in Fig. 12a. As a result, the direct current remains constant, as a battery connected to the PCC takes the power excess. The results of the direct component and the amplitude of the voltage are shown in Fig. 12b and 11b. We can see that the controllers respond very quickly to maintain the

voltage at the reference values between 2s and 3s.

*C. Third scenario: Variation of the irradiance with constant loads*

The performance of the controllers is tested by the variation of the irradiance between 0.5s and 2s, and between 2.35s and 6.65s. The positive sequence component of the currents injected by the inverter is given in Fig. 13a. We notice that the active current is proportional to the active power at the inverter input. This balancing is ensured

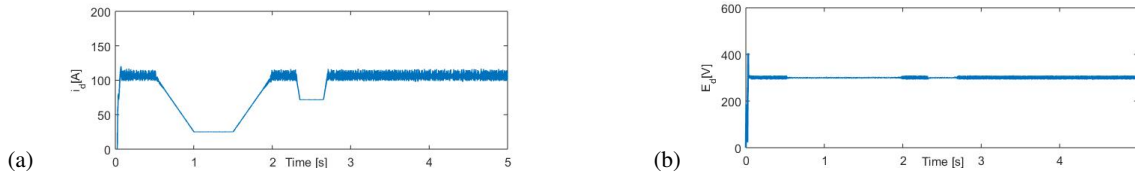


Fig. 13. Direct component of the current (a) and the voltage (b), by considering the third scenario.

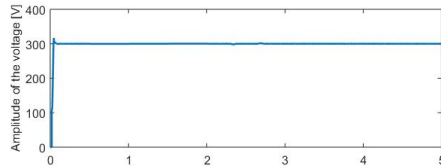


Fig. 14. Voltage amplitude at the PCC by considering the third scenario.

by the battery which is connected at the AC side.

The results of the voltage regulation are presented at Fig. 13b and 14.

#### V. CONCLUSION

The islanded microgrids made with photovoltaic generators are essential in tackling the problems of energy scarcity in Africa. But the intermittent character of the micro-sources and the loads variation can make the systems unstable. To solve these problems, the close control strategy has been devised. This control approach is characterized by a rapid response of controllers to maintain the stable operation of the islanded microgrid. Its performance is analyzed with Matlab/Simulink for a microgrid model made up of one photovoltaic generator, active power loads and elementary distribution system. The results obtained have shown that the controller efficiently maintains the stable operation of the system under the transient solar and the loads power conditions.

#### ACKNOWLEDGMENT

The authors would like to acknowledge the financial support provided by the CIA of UCL.

#### REFERENCES

- [1] H. Jiayi, J. Chuanwen, X. Rong, "A review on distributed energy resources and MicroGrid," *Renewable and Sustainable Energy Reviews*, Vol.12, pp. 2472-2483, 2008.
- [2] E. Hossain, E. Kabalci, R. Bayindir, R. Perez, "A Comprehensive Study on Microgrid Technology," *International Journal of Renewable Energy Research*, Vol.4, No. 4, pp.1094-1107, 2014.
- [3] E.E. Gaona, C.L. Trujillo, J.A. Guacaneme, "Rural microgrids and its potential application in Colombia," *Renewable and Sustainable Energy Reviews* 51, pp.125-137, 2015.
- [4] E. Hossain, E. Kabalci, R. Bayindir, R. Perez, "A Comprehensive Study on Microgrid Technology," *International Journal of Renewable Energy Research*, Vol. 4, No. 4, pp.1094-1107, 2014.
- [5] CIGRE, "Working Group C6.22, Microgrids Engineering, Economics, and Experience," 2015.
- [6] K.S. Rajesh, S.S. Dash, R. Rajagopal, R. Sridhar, "A review on control of ac microgrid," *Renewable and Sustainable Energy Reviews* 71, pp.814-819, 2017.
- [7] L. Rakoa, E. Dvorsky, "Voltage and frequency control for islanded microgrids containing photovoltaic power plants," *Journal of electrical engineering*, Vol. 65, No. 7s, pp.9-14, 2014.
- [8] J. Quesada, R. Sebastin, M. Castro, J.A. Sainz, "Control of inverters in a low voltage microgrid with distributed battery energy storage. Part I: Primary control," *Electric Power Systems Research* 114, pp.126-135, 2014.
- [9] S.G. Malla, C.N. Bhende, "Enhanced operation of stand-alone Photovoltaic-Diesel Generator-Battery system," *Electric Power Systems Research* 107, pp. 250-257, 2014.
- [10] N. S. Jayalakshmi, D. N. Gaonkar, A. Balan, P. Patil, S. A. Raza, "Dynamic Modeling and Performance Study of a Stand-alone Photovoltaic System with Battery Supplying Dynamic Load," *International journal of renewable energy research*, Vol.4, No.3, 2014.
- [11] T. Vigneysh, N. Kumarappan, "Autonomous operation and control of photovoltaic/solid oxide fuel cell/battery energy storage based microgrid using fuzzy logic controller," *International journal of hydrogen energy* 41, pp.1877-1891, 2016.
- [12] N. H. Samrat, N. B. Ahmad, I. A. Choudhury, Z. B. Taha, "Modeling, Control, and Simulation of Battery Storage Photovoltaic-Wave Energy Hybrid Renewable Power Generation Systems for Island Electrification in Malaysia," *Hindawi Publishing Corporation, The Scientific World Journal*, Volume 2014, Article ID 436376, 21 pages.
- [13] S. Verma, H. K. Verma, Md. K. Mohiddin, "Modeling and Analysis of standalone photovoltaic system," *International Journal of Research in Engineering and Technology*, Vol. 02, No. 11, pp.259-265, Nov-2013.
- [14] A. M. Dizqah, A. Maheri, K. Busawon, A. Kamjoo, "Modelling And Simulation Of Standalone Solar Power Systems," *Int. J of Computational Methods and Experimental Measurements*, 2 (1), pp.107-125, 2014.
- [15] Krisadinata, N. Abd. Rahim, H. W. Ping, J. Selvaraj, "Photovoltaic module modeling using simulink/matlab," *Procedia Environmental Sciences* 17, pp.537-546, 2013.
- [16] C. Qi, Z. Ming, "Photovoltaic Module Simulink Model for a Stand-alone PV System," *Physics Procedia* 24, pp.94-100, 2012.
- [17] W. Al-Saedi, S. W. Lachowicz, D. Habibi, O. Bass, "Voltage and frequency regulation based DG unit in an autonomous microgrid operation using Particle Swarm Optimization," *Electrical Power and Energy Systems* 53, pp.742-751, 2013.
- [18] S.G. Malla, C.N. Bhende, "Voltage control of stand-alone wind and solar energy system," *Electrical Power and Energy Systems* 56, pp.361-373, 2014.
- [19] Y. Kircicek, A. Aktas, M. Ucar, S. Ozdemir, E. Ozdemir, "Modeling and Analysis of a Battery Energy Storage System Supplied from Photovoltaic Power Source," *7th International Ege Energy Symposium and Exhibition*, Usak, Turkey, pp.18-20, June 2014.
- [20] O. Tremblay, L. -A. Dessaint, A. -I. Dekkiche, "A Generic Battery Model for the Dynamic Simulation of Hybrid Electric Vehicles," *Vehicle Power and Propulsion Conference*, 2007. VPPC 2007. IEEE, pp.284-289, 2007.
- [21] F. M. Gonzalez -Longatt, "Circuit Based Battery Models: A Review," *2DO congreso iberoamericano de estudiantes de ingeniera elctrica* 2006.
- [22] P. Bhatnagar, R. K. Nema, "Maximum power point tracking control techniques: State-of-the-art in photovoltaic applications," *Renewable and Sustainable Energy Reviews* 23, pp.224-241, 2013.
- [23] X.-Q. Guo, W. -Y. Wu and H.-R. Gu, "Phse locked loop and synchronization methods for gridinterfaced converters: a review," *Przegld Elektrotechniczny (Electrical Review)*, ISSN 0033-2097,R.87NR4/2011,pp.182-187.